ANALYTICAL PROCEDURES

U-Pb dating

U-Pb isotope analyses of the zircons were performed on a Thermo-Elemental VG PlasmaQuad 2 quadrupole-based ICP-MS equipped with an S-option interface and a MicroLas production (Göttingen, Germany) GeoLas 200 CQ laser ablation system utilizing a Lambda Physik (Göttingen, Germany) COMPex 102 ArF excimer laser as a 193 nm deep ultraviolet light source at the Tokyo Institute of Technology. U-Pb isotopic data were obtained from single 20 μm ablation pits with laser repetition rates of 5Hz, a laser ablation time of 15 sec and laser energy density of 5 J/cm^2 at the sample surface. All measurements were corrected using standard standard NIST SRM 610. Because zircon U-Pb data obtained by LA-ICP-MS cannot be perfectly corrected by the calibration using NIST SRM 610 due to the matrix difference (Hirata, 2003, Chemically assisted laser ablation ICP mass spectrometry: Analytical Chemistry, v. 75, p. 228–233), we have used only Pb isotopic data for the discussion. The isobaric interference of ^{204}Hg on ^{204}Pb was corrected by monitoring ^{202}Hg. No common Pb correction was applied to analyses for which the corrected ratio is within 2 sigma error of the uncorrected ratio. Analytical uncertainties include counting statistics and standard deviations of standard analyses during the analytical sessions.

The oldest xenocrystic zircon grain (AC012/07) was also analysed with a SHRIMP II at Hiroshima University. We used a 1.0–1.3 nA mass filtered O_2^- primary ion beam with a ~15 μm analytical spot, and a mass resolution of 5,800 at 1% peak height to separate Hf dioxide peaks from Pb peaks on the mass spectra. One spot analysis consists of 7 cycles. Before the actual analysis, the sample was rastered for 5 minutes in order to remove common Pb on the surface and contamination from the gold coating. The U-Pb ratios were calibrated using ion microprobe standard zircon SL13 (572 Ma). Analytical uncertainties of Pb/Pb ratios are based on counting statistics; those of Pb/U ratios include counting statistics and standard deviation of standard analyses during the analytical sessions. The accuracy of the present ion microprobe technique (including the adequacy of the zircon standard used in this study) was evaluated by dating standard zircon FC1 (1099 Ma; Paces, J.B., Miller, J.D., Jr., 1993, Precise U-Pb ages of Duluth complex and related mafic intrusions, northern Mineeosota: Geochronological insights into physical, petrogenetic, paleomagnetic, abd tectonomagmatic processes associated with the 1.1 Ga midcontinent rift system: Journal

of Geophysical Research, v. 98, p. 13997–14013). The obtained data (Fig. A1) are consistent with the reported results, indicating the analytical validity of the present method.

Trace element analyses

The abundances of Sc, Y, REE and Hf of zircon AC012/07 were measured with the LA-ICP-MS at the Tokyo Institute of Technology, using an ablation pit size of 10 μm, laser repetition rates of 8Hz, a laser ablation time of 10 sec and a laser energy density of 3 J/cm^2 at the sample surface, and the data were normalized against NIST SRM 610.

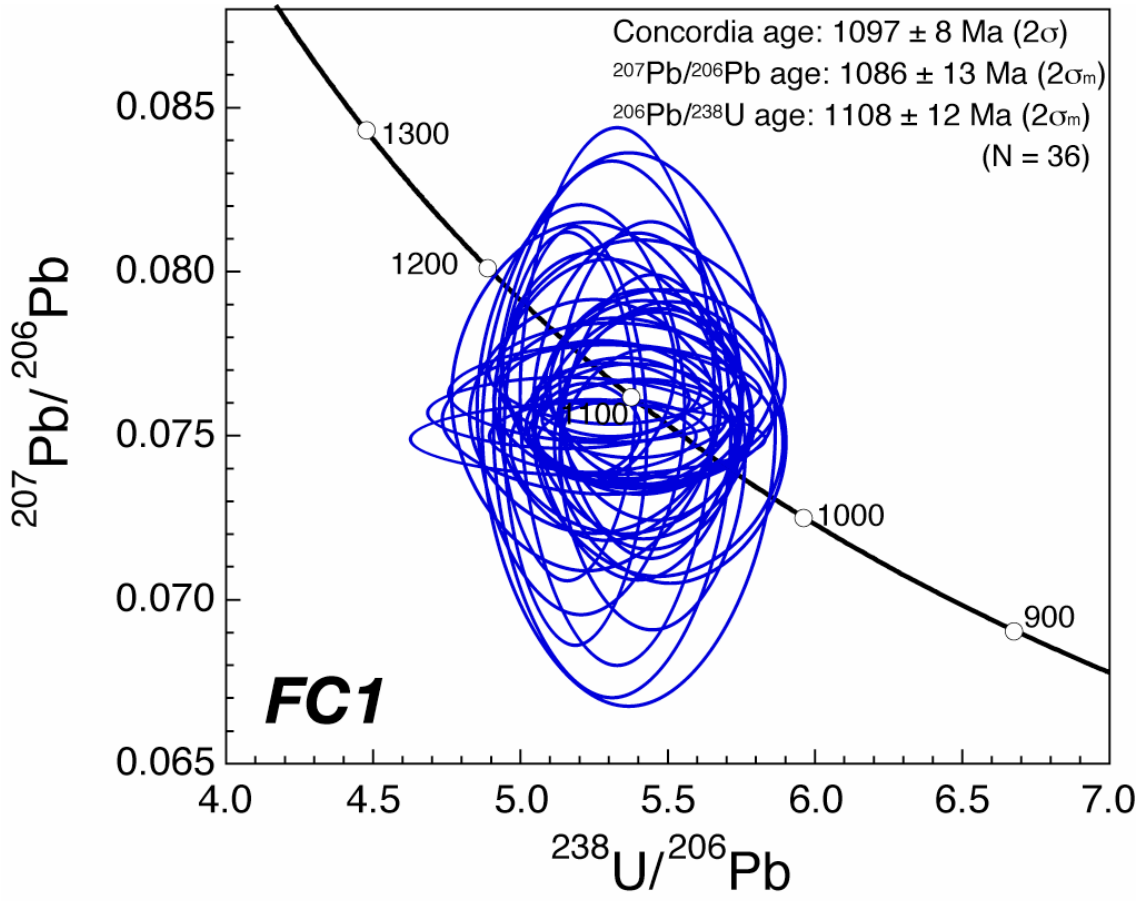

Figure A1. Tera-wasserburg plot of standard zircon FC1. Errors are replicated at 2σ level.

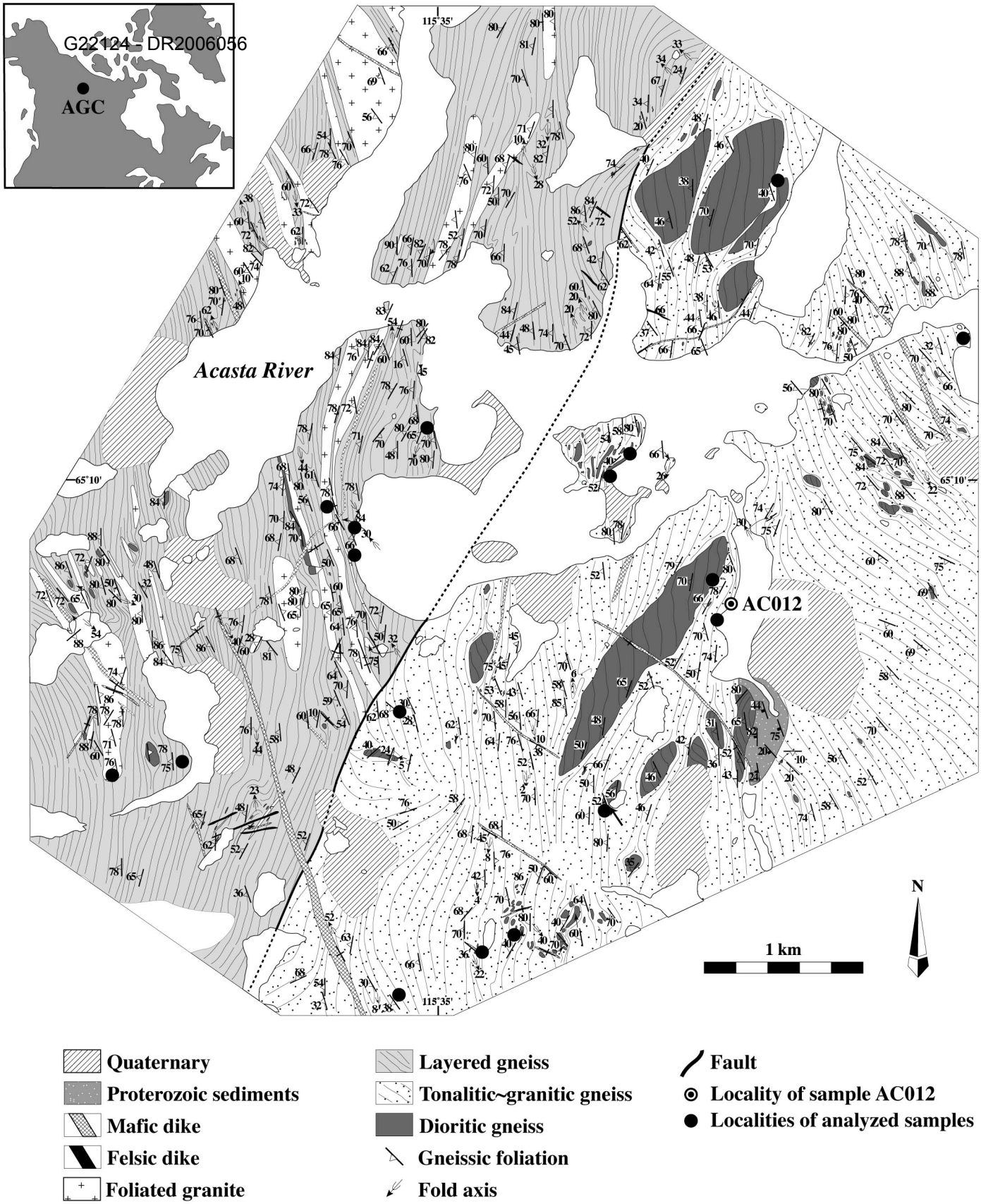

Figure DR1. Geological map of the Acasta Gneiss Complex (AGC) of the Slave Province, northwestern Canada, Canada, based on our own mapping in 2000 and 2002. The location of tonalitic gneiss AC012 is shown, as well as that of other samples which we have analyzed.

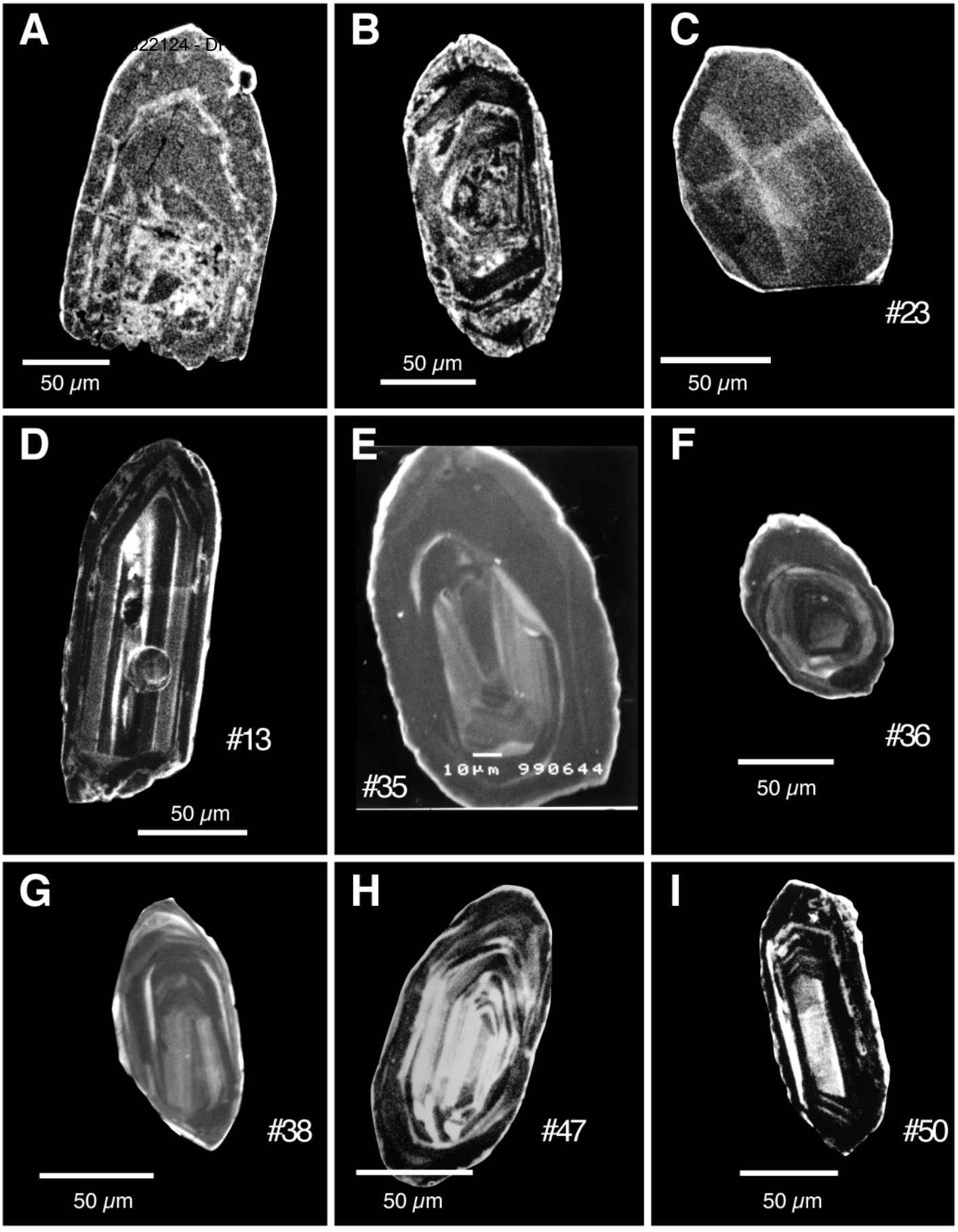

Figure DR2. Cathodoluminescence images of zircons from Acasta gneiss AC012. A: Grain mainly consisting of dark homogenized zircon, infilled by mottled metamict zircon. B: Grain mainly consiststing of mottled metamict zircon. C: Grain AC012/23 mainly consisting of dark zircon, with partly of weakly sector zoned zircon. D–I: Grains showing preserved oscillatory zoning core, mantled by thin (~20 μm) dark overgrowth.

G22124 - DR2006056

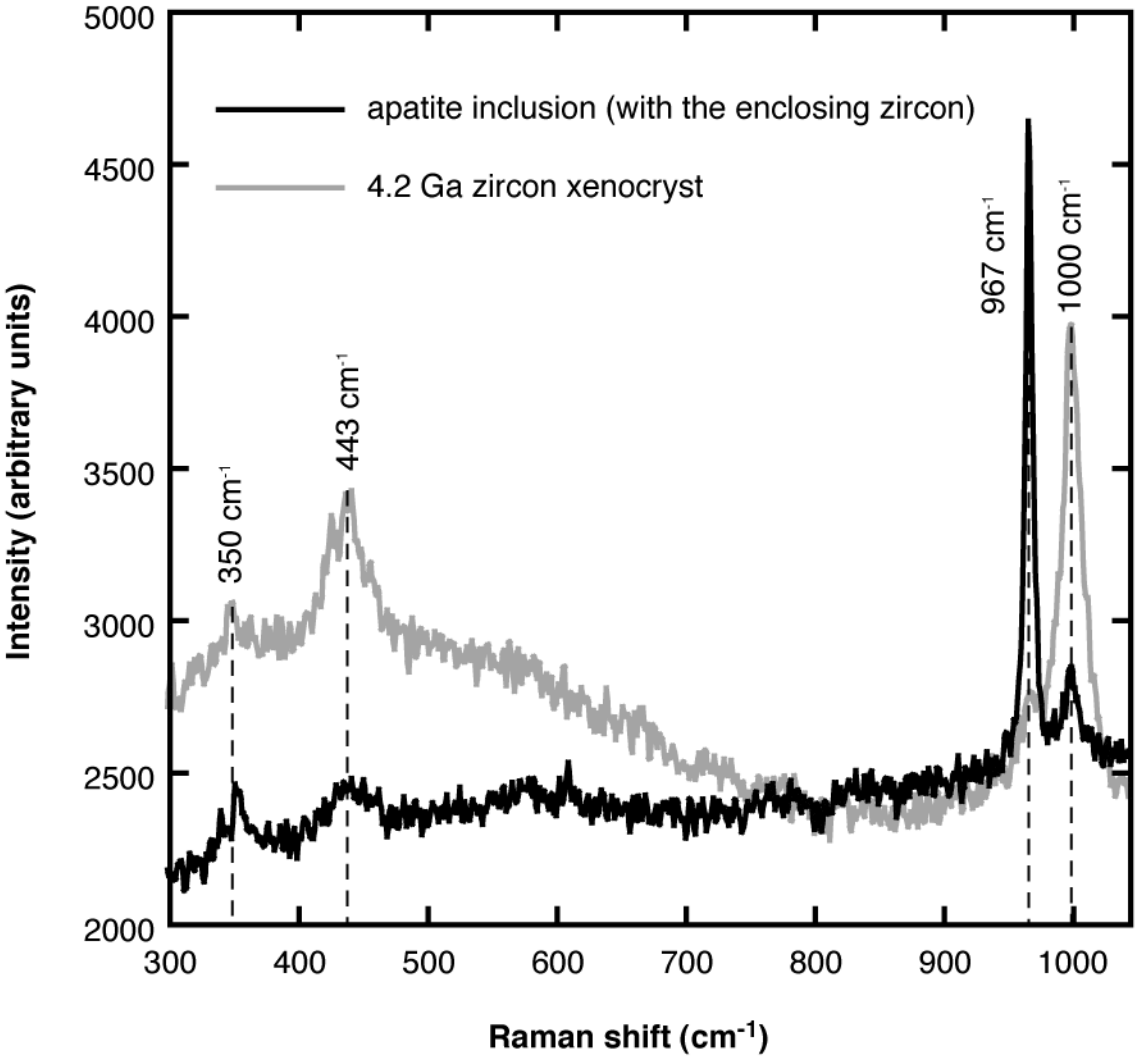

Figure DR3. Raman spectra for an apatite inclusion and its enclosing 4.2 Ga zircon xenocryst from the Acasta gneiss AC012.

TABLE 1 U-Pb-Th AND TRACE ELEMENT DATA FOR AC012/07

U-Pb-Th data

Spot	Method	U (ppm)	Th (ppm)	Th/U	$^{204}Pb/^{206}Pb$	$^{206}Pb^*/^{238}U$	$^{207}Pb^*/^{206}Pb^*$	Age (Ma) $^{206}Pb/^{238}U$	Age (Ma) $^{207}Pb/^{206}Pb$	Disc (%)
1	LA-ICP-MS	N.D.†	N.D.†	N.D.†	0.0002	N.D.†	0.4874 ± 191	N.D.†	4203 ± 58	N.D.†
2	SHRIMP	699	347	0.496	0.0006	0.8611 ± 316	0.4827 ± 150	4004 ± 110	4189 ± 46	4
3	SHRIMP	621	115	0.185	0.0005	0.6900 ± 224	0.3957 ± 32	3383 ± 86	3893 ± 12	13
4	SHRIMP	649	48	0.075	0.0002	0.7567 ± 320	0.3976 ± 76	3632 ± 118	3900 ± 28	7

Trace element data (ppm)

Spot	Sc	Y	Nb	La	Ce	Pr	Nd	Sm	Eu	Gd	Tb	Dy	Ho	Er	Tm	Yb	Lu	Hf
5	396	1196	624	0.1	15	0.2	1.5	9.1	1.3	22	8.0	89	36	155	36	400	54	13621
6	336	547	663	N.D.†	2	0.1	0.5	2.5	0.2	6.5	2.0	37	16	94	28	295	53	16047

Note : Spot numbers correspond to those in Figure 2. Pb* corrected for common Pb using ^{204}Pb. All errors are quoted at 2 σ.

†N.D. = not determined.